Chapter 2: Materials, Synthesis Techniques, Characterization Techniques, and Software used

2.1 Overview

Objective and motivation details about experimental work is discussed in Chapter 1. We have synthesized the Eu^{2+}-doped $CsPbBr_3$ nanocrystal for the various optical study, $CsPbBr_3$ encapsulated Eu-MOF microcrystals for anti-counterfeiting application, $CsPbCl_{1.5}Br_{1.5}$ encapsulated Tb/Eu-MOF microcrystals for WLED application, Er^{3+}, Yb^{3+}: $GdScO_3$ nanoparticles to study the UC mechanism and optical thermometry. In this chapter materials and chemical required are summarized in section 2.2. Different synthesis methods followed for the above mentioned materials are discussed thoroughly section 2.3. The instruments used to investigate the optoelectronic properties of the synthesized samples are briefly discussed in section 2.4. Any properties of the sample are studied, calculated, predicted, or fitted using certain equation or software have been discussed in section 2.5.

2.2 Materials

Materials and chemicals required for the synthesis of different halide perovskites, halide perovskite encapsulated metal-organic frameworks, and lanthanide-doped oxide perovskite are listed in table 2.1. Table includes the materials name, chemical formula, purity of the materials and manufacturer name.

Table 2.1 Materials specifications

S. No.	Chemical Name	Formula	Purity (%)	Manufacturer
1.	Cesium Carbonate	Cs_2CO_3	99.99	Alfa Aesar
2.	Lead (II) Bromide	$PbBr_2$	99.99	Alfa Aesar

3.	Lead Chloride	$PbCl_2$	99.998	Alfa Aesar
4.	Cesium Bromide	CsBr	99.999	Alfa Aesar
5.	Cesium Chloride	CsCl	99.999	Alfa Aesar
6.	Europium (II) Oxide	Eu_2O_3	99.99	Alfa Aesar
7.	Terbium (III) Oxide	Tb_2O_3,	99.99	Alfa Aesar
8.	Gadolinium (III) Oxide	Gd_2O_3	99.9	Alfa Aesar
9.	Scandium (III) Oxide	Sc_2O_3	99.99	Alfa Aesar
10.	Ytterbium (III) Oxide	Yb_2O_3	99.99	Alfa Aesar
11.	Erbium (III) Oxide	Er_2O_3	99.9	Alfa Aesar
12.	Nitric Acid	HNO_3	69.0	Merck
13.	Aminoacetic Acid	NH_2CH_2COOH	99.0	Thermo Fisher
15.	Hydrobromic Acid	HBr	47.0	Spectrochem
16.	Oleic Acid	$C_{18}H_{34}O_2$	90.0	Alfa Aesar
17.	1,3,5 Benzene-Tricarboxylic Acid	$C_9H_6O_6$	98.0	Thermo Fisher
18.	Poly (methyl methacrylate)	$(C_5H_8O_2)_n$	-	Thermo Fisher
19.	Oleylamine	$C_{18}H_{37}N$	-	Sigma-Aldrich
20.	1-Octadecene	$CH_3(CH_2)_{15}CHCH_2$	-	Alfa Aesar
21.	N, N-Dimethyle formamide	$HCON(CH_3)_2$	99.0	EMPCURA
22.	Dimethyle Sulfoxide	$CH_3)_2SO$	99.0	EMPCURA
23.	n-Hexane	$CH_3(CH)_4CH_3$		Alfa Aesar
24.	Ethanol	C_2H_6O	99.9	Qualigens
25.	Mehanol	CH_3OH	99.0	Qualigens
26.	Propan-2-ol	$CH_3CH_2CH_2OH$	99.0	Thermo Fisher
27.	Acetone	CH_3COCH_3	99.0	Merck

2.3 Synthesis Techniques

All the available methods to synthesized the bulk or nanomaterials are categorized into top-down and bottom-up approach. In all experimental work discussed in subsequent

Chapters, bottom up approach have been followed. These include hot-injection method, solution processed hydrothermal method, and self-propagated gel-combustion method discussed in section 2.3.1, 2.3.2, and 2.3.3, respectively.

2.3.1 Hot-Injection Method

Hot-injection method is the very widely used synthesis techniques for the halide perovskites, particularly lead based halide perovskite [30]. This is two-steps synthesis method. In the first step, the Cesium-oleate has been prepared as stock solution. In second step, Cesium-oleate stock solution is quickly injected into the lead-halide (PbX_2; X=Cl, Br, I) solution at temperature around 120 ºC to form the final product ($CsPbX_3$) and hence named hot-injection. Procedural schematic is shown in Fig. 2.1.

2.3.1.1 Synthesis of Synthesis of $CsPbX_3$ (X= Cl, Br, I)

Step 1: Synthesis of cesium-oleate stock solution: Initially, 1-Octadecene (ODE, 30 mL) and oleic acid (OA, 2.5 mL) was added to the Cs_2CO_3 (0.82g), that was kept in a 3-neck round bottom flask under inert environment (Argon gas purging). Solution's temperature was then raised to 120°C and kept maintained with constant stirring until a homogenous Cesium-oleate solution formed. This obtained solution is now referred as stock solution for the next step, which has the self-life up to three months.

Step 2: Synthesis of $CsPbX_3$ (X= Cl, Br, I): Required stoichiometry of PbX_2, 15 mL of ODE, 1 mL OA, and 1 mL oleylamine (OAm) was initially loaded in a 3-neck round-bottomed flask, that placed on hot plate equipped with a magnetic stirring. This solution was then dried at 120°C under Argon gas inert environment for 30 minutes. Furthermore, the solution temperature was adjusted till the PbX_2 was completely dissolved. Subsequently, the pre-

heated (120°C) Cesium-oleate stock solution was swiftly injected by a syringe into the 3-neck round-bottomed flask containing PbX_2 solution. After few seconds, this solution was abruptly cool down to room temperature in ice bath to stop the reaction. The obtained solution was centrifuged to discard the supernatant and washed several times. The obtained final particle is now dispersed in n-hexane for further characterization.

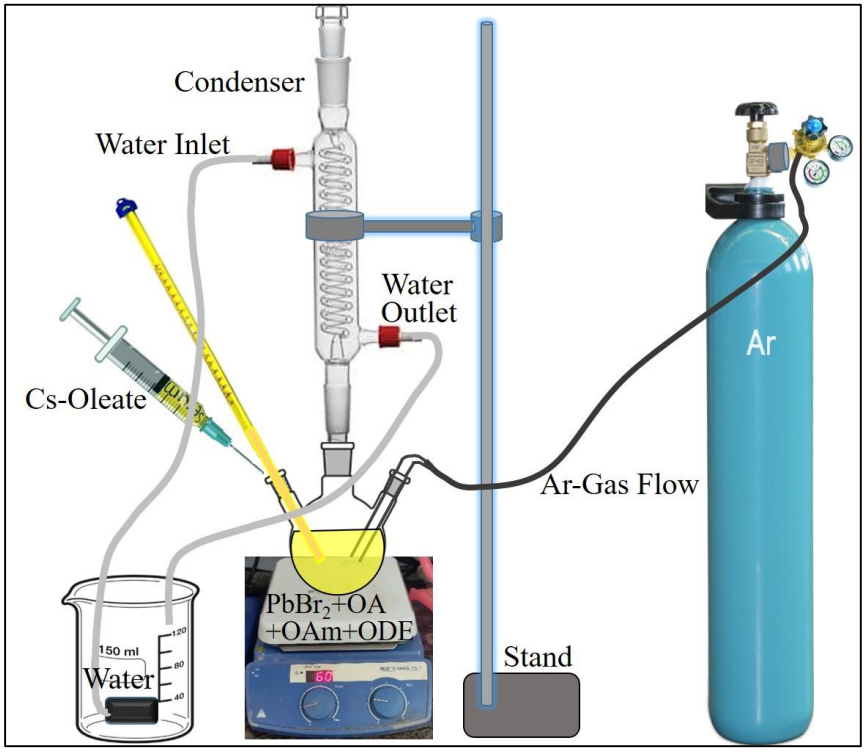

Figure 2.1: Hot-injection synthesis technique for halide perovskite.

2.3.1.2 Synthesis of Ln-doped $CsPbX_3$

For the synthesis of Ln-doped $CsPbX_3$, the required amount of Ln_2O_3 was first transformed into LnX_3 using dilute HX acid, or directly LnX_3 precursor being used. Then LnX_3 precursor solution is added to the PbX_3 solution containing 15 mL of ODE, 1 mL OA, 1 mL OAm. While other procedures were implemented as discussed in step-2.

2.3.2 Solution-Processed Hydrothermal Method

Solution-processed hydrothermal method is the well explored bottom-up technique to synthesize the uniform nano and well as micro particles. In this method all the precursors are initially dissolved in a particular solvent separately. Then all the precursors solutions are uniformly mixed in a beaker and then transferred into the Teflon-lined stainless steel autoclave [110]. The autoclave is kept in a furnace at desired time and temperature to grow the particles. Grown particles are separated using centrifugation and dried for the further characterizations. Here this method has been used for the synthesis of inorganic halide perovskite encapsulated Ln-MOFs.

2.3.2.1 Synthesis of Ln-MOF

The $Ln(NO_3)_3$ is obtained by the reaction of Ln_2O_3 and HNO_3. To obtain $Ln(NO_3)_3$, weighted amount of Ln_2O_3 is taken in a beaker and the required amount of HNO_3 is added into it. The solution is stirred for 1 hour at 200 rpm, a temperature of 40 ºC to obtain a clear transparent nitrate solution. Then, the temperature is increased to remove the excess HNO_3. Further, 5 mL DMF solution is added into it and stirred to obtain the clear transparent solution. In another beaker containing 15 mL of DMF, required amount of organic linker 1,3,5 benzene-tricarboxylic acid (H_3BTC) is added and stirred at 40 ºC for 1 hour at 200 rpm to get a perfectly dissolved solution. Then, both the solutions (DMF solution of $Ln(NO_3)_3$ and H_3BTC) are mixed in a beaker and is ultra-sonicated for 10 minutes to obtain a homogeneous mixture. This solution is then transferred into a Teflon-lined stainless steel autoclave and kept in a furnace at 120 ºC for 48 h [111]. Then, it is centrifuged at 7000 rpm and washed several times using ethanol. Particles are separated and dried in a vacuum oven maintained at 80 ºC for 12 h for further characterizations. All these synthesis steps are depicted in Fig. 2.2.

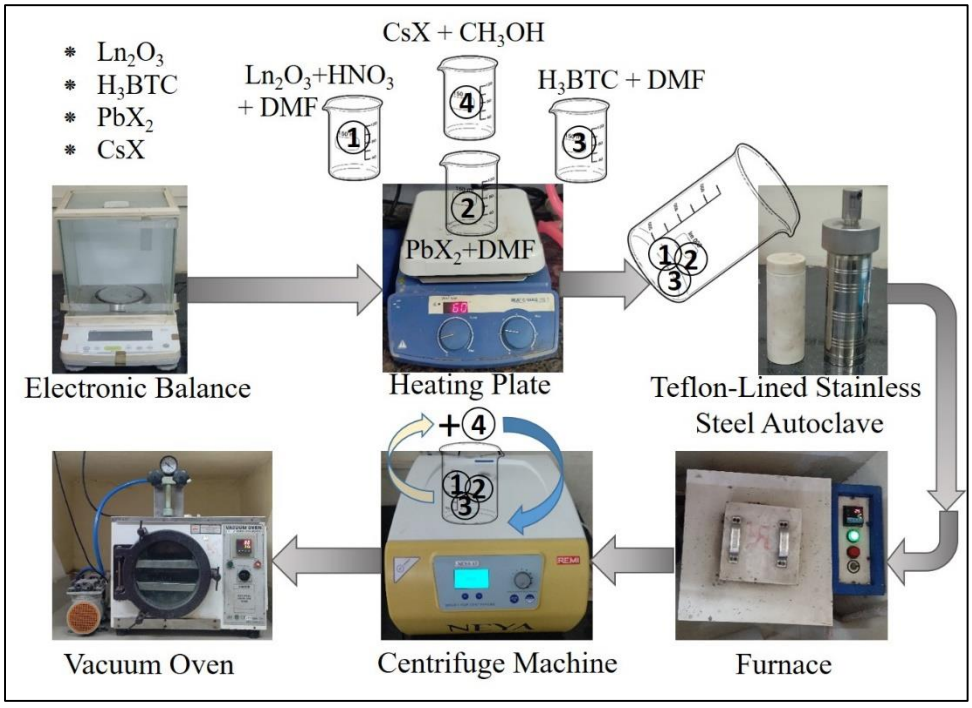

Figure 2.2: Synthesis procedure of metal-organic framework.

2.3.2.2 Synthesis of $CsPbX_3$@Ln-MOF

For the synthesis of $CsPbX_3$@Ln-MOF initially PbX_2@Ln-MOF has been synthesized. Synthesis steps and precursors are followed as for Ln-MOF discussed earlier, only an extra precursor PbX_2 dissolved in 5 mL DMF solution. In separate beaker required amount of CsX is dissolved in 6 mL of methanol and 2 mL of DI water kept at 40 ºC for 30 minutes. Thus, obtained PbX_2@Ln-MOF powder is mixed in a beaker containing CsBr solution. It is stirred for 10 minutes at 40 ºC with 200 rpm for uniform mixing to get the $CsPbBr_3$@ Eu-MOF. Then, it is centrifuged at 7000 rpm and washed several times using ethanol. Particles are separated after centrifugation and dried in a vacuum oven maintained at 80 ºC for 12 h. Finally, $CsPbX_3$@Ln-MOF powder obtained is used for further characterization and analysis.

2.3.3 Self-Propagated Gel-Combustion Method

Self-propagated gel-combustion method is one of the cost effective methods to synthesize particles in the nano-regime [112]. In this method, nitrate solution of each metal is prepared and mixed with required amount of glycine or citric acid that act as fuel for the combustion reaction. This does not require costly equipment and synthesis can be done in open environment. However, concerning the safety issues, the reaction is performed in closed chamber.

Synthesis of M′M″O_3 and Ln^{3+}: M′M″O_3: M′M″O_3 is synthesized through the self-propagated gel-combustion technique taking oxide of each metals as a precursor [113]. The pictorial representation of the synthesis steps is shown in Fig. 2.3. The calculated amount of M′$_2O_3$ and M″$_2O_3$ were weighed and dissolved in a required amount of HNO_3 to obtain metal nitrate. For the combustion reaction, glycine or citric acid can be taken as a fuel. In a 50 mL beaker, both the nitrates metal precursors were taken and then heated at 150 °C to get completely dissolved transparent mixture solution. After approximately 30 minutes, bubble formation was observed, and the solution began to transform into a gel-like viscous liquid. Subsequently, the temperature was increased to 250 °C, triggering ignition and resulting in a foam-like residue. This residue was then ground into a powder using an agate mortar for further characterization and analysis.

The preparation techniques of Ln^{3+}-doped M′M″O_3 are same as discussed above. Each Ln_2O_3 is dissolved in required amount of HNO_3 to obtained Ln-nitrate. Ln-nitrate is then mixed with metal-nitrate and glycine solution. Subsequent steps are same as discussed for the M′M″O_3. This is employed to synthesize the Yb^{3+}, Er^{3+}: $GdScO_3$ nanocrystal for the optical thermometry discussed in chapter 6.

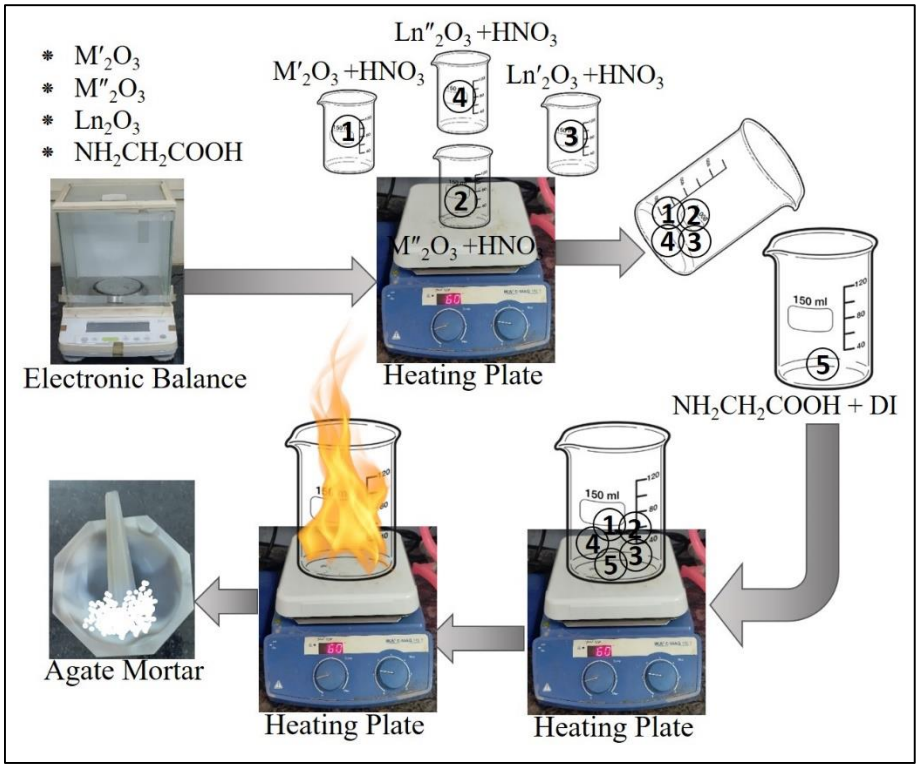

Figure 2.3: Pictorial representation of the synthesis steps of self-propagated gel-combustion method.

2.4 Characterization Techniques

2.4.1 X-ray diffraction (XRD)

XRD is used to study the phase and structure of the synthesized sample as well as other structural characteristics of the materials, such as average crystallite size and crystallinity [114]. It is a flexible and non-destructive analytical method. All the XRD patterns have been recorded using a MiniFlex 600 diffractometer, Rigaku, Japan equipped with Cu as a source of X-ray. Cu Kα radiation of wavelength 1.5056 Å was used for the diffraction (shown in Fig. 2.4(b). Here, to produce the X-rays, applied voltage is 40 kV and a current of 15 mA [115]. X-ray beam is incident on the sample and the diffracted beam is collected by the detector. X-ray diffraction from the crystal plane is shown in Fig. 2.4. Constructive interference of a monochromatic X-ray beam, scattered at specific angles from a series of

lattice planes in a material, results in the formation of XRD peaks in the diffraction pattern. The XRD method analyzes several properties of the polycrystalline or single crystal material by using Bragg's law ($2d\sin\theta = n\lambda$), where d is the distance between the structural planes, n is the order of the diffraction pattern, θ is the scattering angle, and λ is the X-ray wavelength. Diffraction pattern's data are collected in a step size 0.02° in the range $10° \leq 2\theta \leq 90°$ with scanning rate 5°/min. The atomic positions inside the lattice planes identify the peak intensities. Whereas the full width at half maximum (FWHM) of the peak is proportional to the crystallite size of the sample.

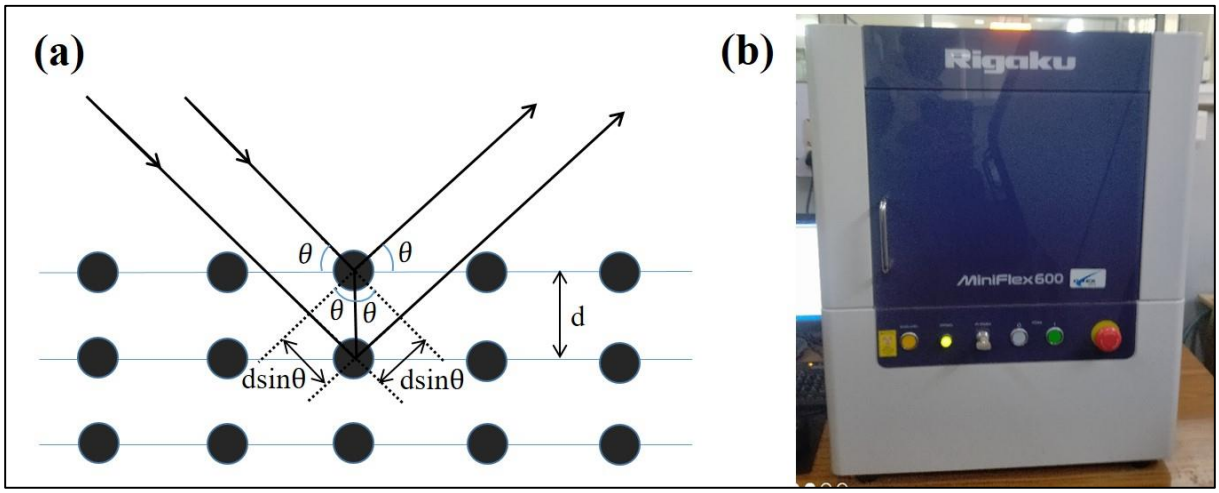

Figure 2.4: (a) X-ray diffraction through crystal planes, (b) X-ray diffractometer (MiniFlex 600, Rigaku, Japan), CIF IIT (BHU).

Lebail analysis using the FullProf software of the XRD data gives the lattice parameters a, b, and c, as well $\alpha,\ \beta, \gamma$ of the unit cell of the sample. Integrating this study to Rietveld analysis provide the information of the position of the constituent atoms in the unit cell.

2.4.2 Scanning Electron Microscopy (SEM)

SEM is used to determine the particle morphology, size up to the nm scale, and elemental mapping of the sample [116]. In all SEM characterizations, EVO - Scanning

Electron Microscope MA15/18, CARL ZEISS MICROSCOPY LTD is used. The electron emission source is tungsten filament operating at 20 kV. Electrons from the tungsten filament are incident on the specimen after passing through the magnetic lenses (ray-diagram is shown in Fig. 2.5).

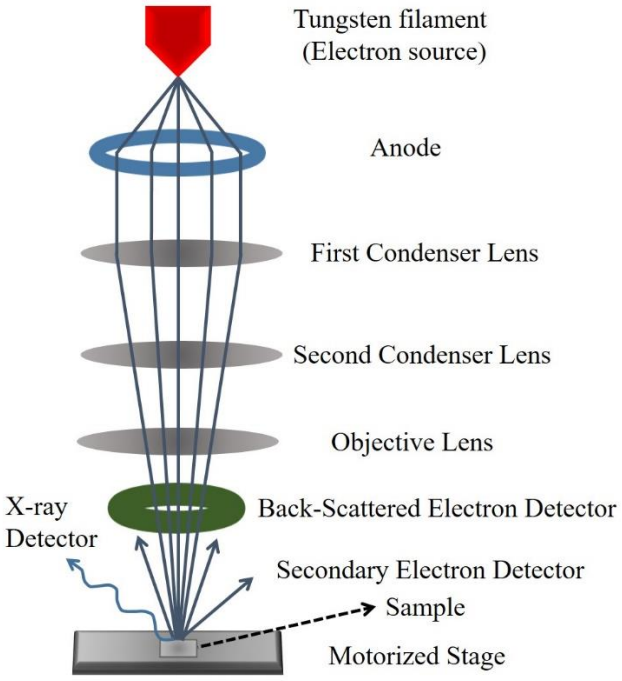

Figure 2.5: Ray-diagram of SEM and its major components.

A few incident electrons are backscattered, some of them generate secondary electrons, and a few of them generate X-ray radiation. Secondary electrons are more abundant than the backscattered electrons. Imaging is performed by the secondary and backscattered electrons detected by the detectors. Both secondary and backscattered electrons are detected through the Everhart-Thornley detector that consist of positively charged biased grid. Digital photograph of the EVO – SEM MA15 / 18, CARL ZEISS is shown in Fig. 2.6.

Figure 2.6: Digital photograph of the EVO – SEM MA15 / 18, CARL ZEISS (CIF, IIT BHU).

This instrument also facilitates the elemental analysis of the sample by the principle energy-dispersive X-ray spectroscopy (EDS). For EDS, 51N1000 – EDS system, Oxford Instruments Nanoanalysis, is used. For the EDS spectrum, generated X-ray radiation is only used. The spectrum consists of peaks corresponding to each element present in the sample. This provide the initial confirmatory test of the presence of the constituent elements in the sample.

2.4.3 High Resolution-Transmission Electron Microscopy (HR-TEM)

HR-TEM is also used to determine the morphology and particle size of the sample [117]. It is very useful for the sample of particle size below 20 nm. For the HR-TEM measurement, sample is uniformly dispersed in particular solution (ethanol, propanol, acetone, toluene, n-hexane, etc.). Then it is drop-cast on a carbon-coated copper grid (3 mm diameter, 300-mesh). The grid is vacuum - dried to avoid any contaminations and then taken for the analysis. Ray-diagram of the TEM is shown in Fig. 2.7 (left). The electron transmitted through the sample is used for the imaging.

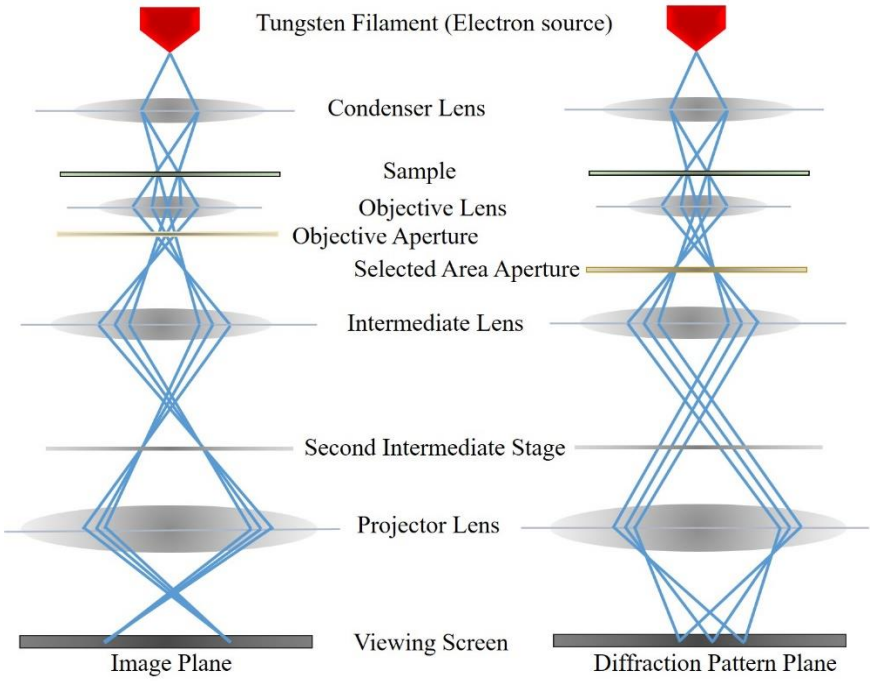

Figure 2.7: Ray diagram of TEM for imaging (left) and selected area diffraction pattern measurement (right).

For the HR-TEM analysis Tecnai G2 20 TWIN, FEI Company of USA (S.E.A.) PTE, LTD has been used. Digital photograph of HR-TEM Tecnai G2 20 TWIN is shown in Fig. 2.8.

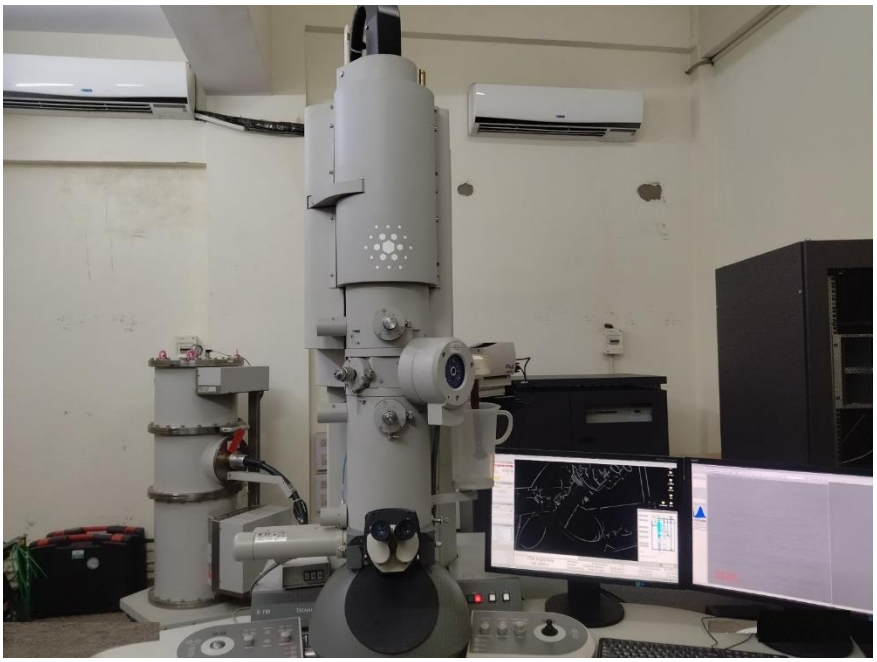

Figure 2.8: Digital photograph of Tecnai G2 20 TWIN, HR-TEM setup (CIF IIT BHU).

For the measurement of selected area electron diffraction (SAED) pattern system is equipped with Octane Plus SDD detector, EDAX Inc. Ray diagram for the SAED pattern measurement is shown in Fig. 2.7 (right). For the imaging objective aperture is employed, whereas for the SAED pattern, selected area aperture is used. SAED patterns help to predict the amorphous, and crystallinity of the samples.

2.4.4 Brunauer-Emmett-Teller (BET) analysis

Brunauer-Emmett-Teller (BET) is a widely used method for the analysis of the surface area and porosity of materials such as metal organic framework (MOF) [118]. It involves measuring the amount of gas (usually nitrogen or argon) adsorbed onto the surface of a material at various relative pressures and then BET equation is to calculate the specific surface area.

Figure 2.9: Digital photograph of BET measurement setup (CIF, IIT BHU).

Initially, the sample is typically degassed at elevated temperatures to remove any adsorbed contaminants. The sample is then cooled to the adsorption temperature, usually that of liquid

nitrogen (77 K). The sample is exposed to a N_2 gas, at various relative pressures (P/P_0). The amount of gas adsorbed is measured at each relative pressure to create an adsorption isotherm. The BET equation is applied to the linear portion of the adsorption isotherm.

$$\frac{P}{V_a(P_0 - P)} = \frac{1}{V_m C} + \frac{C-1}{V_m C}\frac{P}{P_0} \quad \ldots (2.1)$$

Where, P is the pressure of the gas and P_0 is the saturation pressure of the gas at the adsorption temperature. The adsorbed volume of the gas is represented by V_a. The C is proportional to the exponential of the reduced surface adsorption energy, V_m is the effective monolayer capacity. The BET surface area is determined by the equation-

$$S_{BET} = V_m A \quad \ldots (2.2)$$

The constant A is the cross-sectional area of N_2 molecule (0.162 nm^2). For mesoporous materials (2-50 nm), pore size distribution can be analyzed using methods such as Barrett-Joyner-Halenda (BJH) applied to the desorption branch of the absorption-desorption isotherm.

2.4.5 X-Ray Photoelectron Spectroscopy (XPS)

XPS is a surface analysis technique up to 1-10 nm. It is used to determine the chemical composition of the surface, elemental composition, oxidation state of the elements, and the concentration of the elements within 1-10 nm range [119]. This technique uses thin film or pallet of 5 – 10 mm diameter. The sample is placed in a high to ultra-high vacuum chamber (10^{-8} – 10^{-9} millibar). Then, the sample inside the chamber is irradiated by the X-ray beam (for Al Kα X-ray energy is 1486.6 eV) and number of emitted electrons and their kinetic energy are assessed. This gives the XPS survey spectrum consisting of characteristic sharp

peak of the elements with varying intensity. The schematic of the XPS analysis is shown in Fig. 2.10.

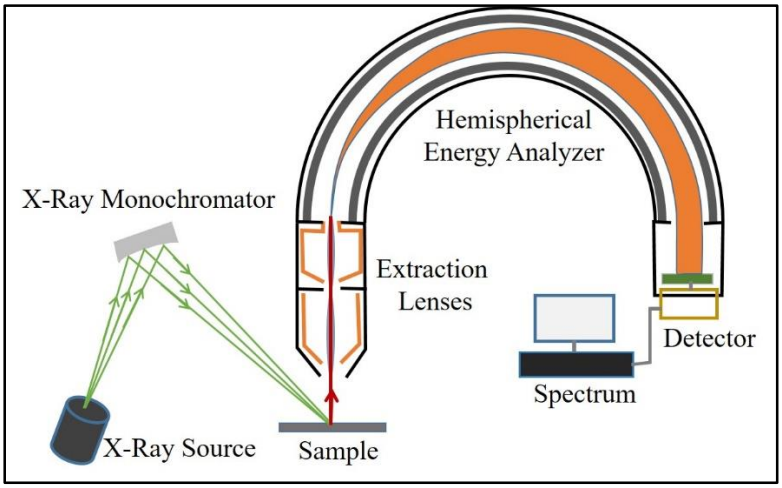

Figure 2.10: Schematic diagram of the XPS analysis.

Kinetic energy of the emitted electron gives the information of binding energy which is the characteristic of specific elements and hence elemental composition can be investigated. In XPS spectrum peak position and shape are the signature of chemical composition, oxidation state, and binding structure. Whereas, peak intensity helps to determine the element concentration.

Figure 2.11: Digital photograph of K-Alpha Thermo Fisher Scientific XPS setup (CIF, IIT BHU).

For the XPS measurement K-Alpha Thermo Fisher Scientific setup is used and its digital photograph is shown in Fig. 2.11. In the XPS spectrum, s-orbital electrons correspond only one peak. Whereas for the p, d, or f orbital electrons two peaks appear. Peaks are assigned accordingly the n (principle quantum number), *l* (orbital quantum number) and j (j = *l* + s, spin angular momentum number, s = $\pm$ 1/2) value. Thus for the p orbital electron peaks are assigned as $p_{1/2}$ and $p_{3/2}$, for d-orbital electrons, $d_{3/2}$ and $d_{5/2}$, and for electron in f orbital $f_{5/2}$ and $f_{7/2}$. The intensity ratio of the peaks that is proportional to the splitting is 1:2, 2:3, and 3:4, respectively for the p, d, and f orbital electrons.

2.4.6 Ultra Violet (UV) –Visible-near Infrared (NIR) Spectroscopy

UV-visible-NIR spectroscopy is a powerful technique for the analysis of absorption transitions and optical bandgap of the sample [120]. It uses deuterium (D2) lamp as a radiation source for the UV-region and tungsten lamp for the visible and near-infrared region. Charge coupled device (CCD) or photomultiplier tube (PMT) is used for the detection purpose. The ray diagram of the UV-visible spectroscopy analysis is shown in Fig. 2.12(a). Light from the source passes through the monochromator, which gives monochromatic light at the exit. Light is split into two path; one falls on the sample and other as a reference beam. Then both the beam reaches the detector. The parametric difference between the reference and the beam encounters the sample gives the absorption transition of the sample. Law of UV-visible-NIR absorption spectroscopy is given by Beer and Lambert collectively called Beer-Lambert's law. This law says that the light absorption by the material is proportional to the concentration and optical path length.

$$A = \log_{10}\left(\frac{I}{I_0}\right) = \varepsilon \times c \times l \qquad \ldots (2.3)$$

Where, A is the absorbance, ε is the absorptive coefficient, c is the concentration of the sample, and l is the optical path length. I_0 and I are, respectively, the incident and transmitted light intensity.

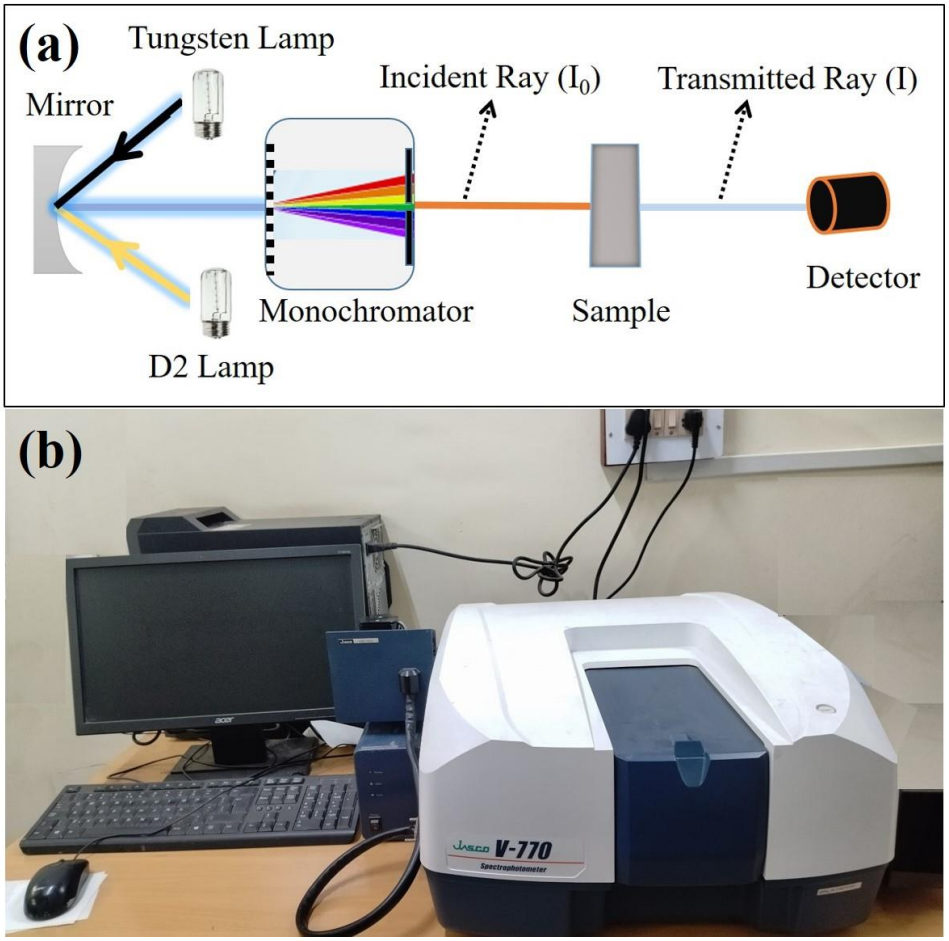

Figure 2.12: (a) Ray-diagram of the UV-visible absorption analysis. (b) Digital photograph of JASCO V770 UV-Visible spectrophotometer (Department of Physics, IIT BHU).

All the UV−visible-NIR absorption spectroscopy studies are done using a JASCO V770 spectrophotometer, digital photograph is shown in Fig. 2.12(b).

The optical bandgap of the material is determined by the Tauc-plot using Tauc equation.

$$(\alpha h\nu)^{1/n} = A\left(h\nu - E_g\right) \quad \ldots (2.4)$$

Where E_g, is the optical bandgap, α is absorption coefficient, A is the constant, and $h\nu$ is the incident photon energy. Mode of transition is determined by the '1/n'. For the direct allowed it is 1/2, and for direct forbidden it is 2/3. The '1/n' value for the indirect allowed and indirect forbidden is 2 and 3, respectively.

2.4.7 Fourier Transform - Infrared (FT-IR) Spectroscopy

FT-IR spectroscopy is related with the lattice vibration and vibrational motion of the covalent bonded molecules after the interaction the IR light [121]. It gives quantitative and qualitative information of the chemical bonding though the scattered, reflected or transmitted IR radiations. IR spectrometer consist of mainly IR source, sample compartment, and a detector. Through a mathematical process called Fourier transformation, the output information of radiation intensity as a function of time is decoded into frequency and intensity.

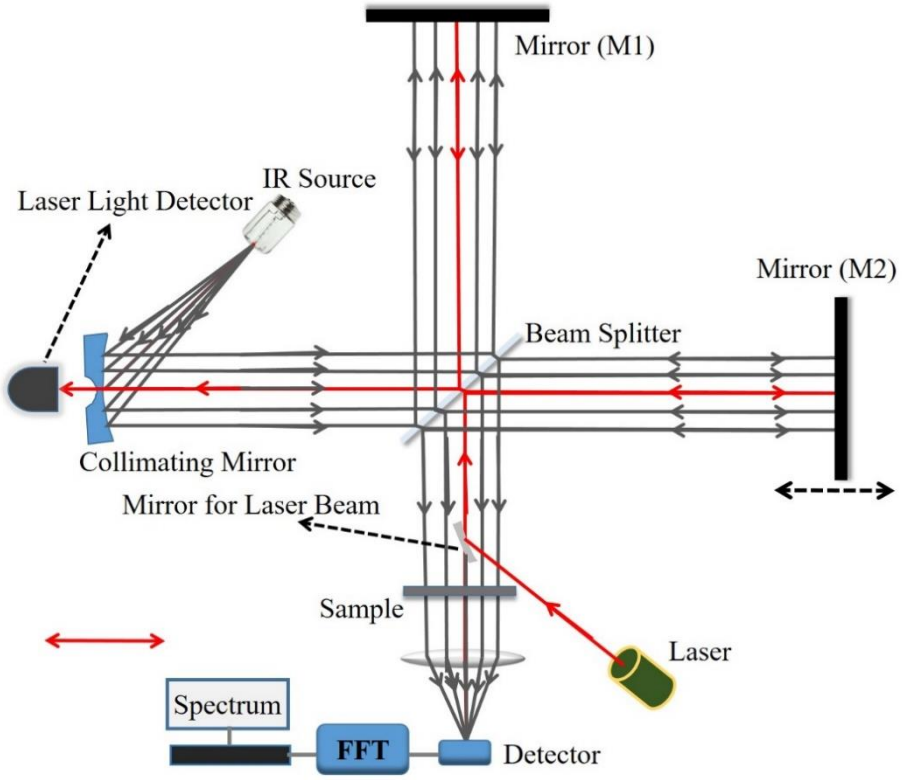

Figure 2.13: Ray diagram of FT-IR spectroscopy.

The ray diagram of the FTIR spectroscopy is shown in Fig. 2.13. If optical path difference is integral multiple of wavelength, then maxima is form and if it is odd integral multiple of half-wavelength then minima occur. The moving mirror's position is tracked and the timing of data collection is established by the interferometer using the interferogram. Since the laser radiation is thought to be almost monochromatic, or to have no linewidth, the interferogram it produces is a well- defined sinusoidal wave that does not decay with a significant amount of retardation. Therefore, every unique point on the interferogram, including its maxima, minima, and zero-crossing points, that can be used to calculate the location of the moving mirror. Combined beam from the interferogram is encountered on to the sample and various phenomena such as absorption, reflection, scattering, etc., occur. This optical signal is detected by the detector, then converted into electrical digital one, and finally Fourier transformed into a spectrum.

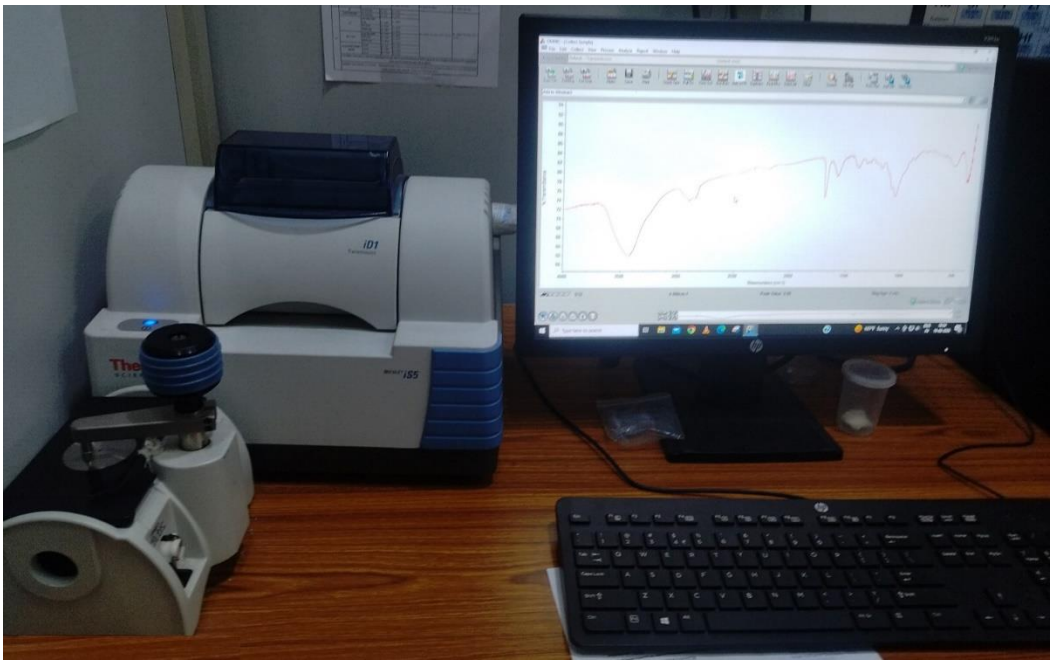

Figure 2.14: Digital photograph of Nicolet iS5, Thermofisher (CIF, IIT BHU).

In all FT-IR spectra, we have record the data in the mid IR region between 4000 – 400 cm^{-1} with Nicolet iS5, Thermofisher. Digital photograph of the setup is shown in Fig. 2.14. Popular continuous IR source are Nernst glower (made up of rare-earth oxides), Globar (silicon carbide), and Nichrome coil. Among these, Nernst glower is most commonly used. The IR spectrometers uses either thermal detectors or photon detectors. Thermal detectors consist of thermocouples (voltage at junction of dissimilar metals), thermistors (electrical resistance: For the mid IR region deuterated tri-glycine sulfate (DTGS) pyroelectric detector is the universal one; in the 700 – 10 cm^{-1} Si-bolometer is used), and Golay detectors (expansion of a non-absorbing gas). Whereas, photon detectors employ the interaction of IR radiation with semiconductor materials (array diode detector).

2.4.8 Photoluminescence (PL) Spectroscopy

This is a versatile instrument for optical characterization. Main part of the PL spectrometer is light source (Xenon lamp, 450 W), monochromator, sample compartment, and detector (photomultiplier tube: PMT) [5]. Ray diagram consisting of main components is shown in Fig. 2.15. Light from the xenon lamp falls into the entrance slit of the monochromator (say excitation monochromator). Monochromator consist of grating and mirror arranged in a particular fashion to give the desired monochromatic light at the exit slit. This monochromatic light is incident on the sample that excite the sample and emitted photons are directed towards the second monochromator (say emission monochromator). At the exit slit, detector (PMT) is coupled to detect the emitted photons and finally to the electronic circuit to record the spectrum. PMT consist of dynode to amplify the week-signal to be recorded.

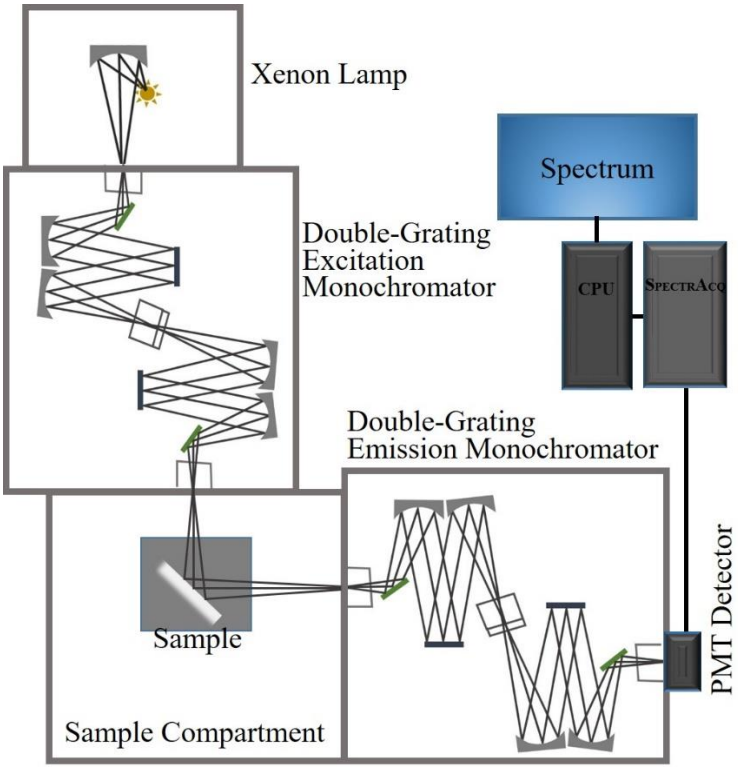

Figure 2.15: Ray-diagram of Fluorolog-3 spectrophotometer.

Figure 2.16: Digital photograph of Horiba Fluorolog-3 spectrophotometer (Department of Physics, IIT BHU).

All the PL analysis have been done using the Horiba Fluorolog-3 spectrophotometer shown in Fig. 2.16. We record photoluminescence excitation (PLE) spectrum for an emission peak to predict the absorption transition in molecule (band to band) or ions (ground state to excited state). The ions or electrons in the excited state come back to the ground state by releasing photons depicted by the emission spectrum. This provide the initial guess of the optical bandgap of the material, purity, composition and concentration, etc.

2.4.9 Time resolved photoluminescence spectroscopy (TRPL)

Time-Resolved Photoluminescence (TRPL) decay analysis is a technique used to study the dynamics of excited states in materials and biological systems [122]. By measuring the decay of photoluminescence as a function of time after excitation, various processes such as carrier recombination, energy transfer, and non-radiative decay mechanisms can be obtained. In TRPL, a short laser pulse is used to excite the sample. The intensity of the emitted light is measured as a function of time following a short excitation pulse. This allows the determination of the decay time of the photoluminescence emission, which provides information about the lifetimes of excited states.

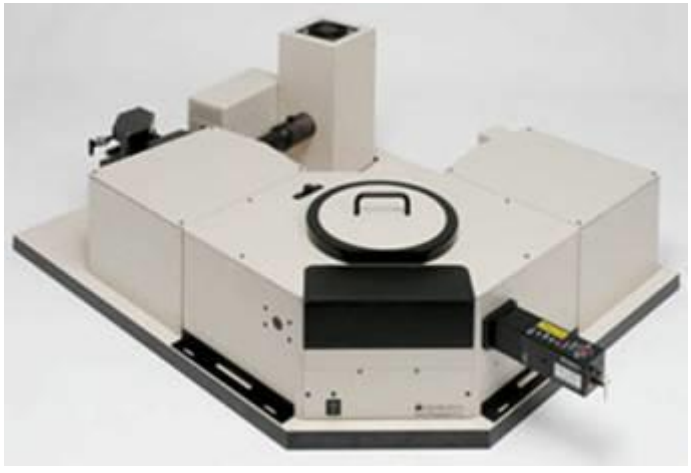

Figure 2.17: Digital photograph of FLS980 Edinburgh spectrometer.

All the PL decay analysis is performed by a pulsed diode as the excitation source attached with FLS980 Edinburgh spectrometer as shown in Fig. 2.17.

The decay of photoluminescence can be characterized by different types of dynamics, depending on the material and the processes involved. For a single exponential function decay, the PL intensity variation is given as

$$I(t) = I_0 e^{-t/\tau} \quad \ldots (2.5)$$

Where *I(t)* is the PL intensity at time *t*, I_0 is the initial intensity, and τ is the decay time or lifetime of the excited state. The PL intensity variation in higher exponential decay is expressed as

$$I(t) = \sum_i A_i \, e^{-t/\tau_i} \quad \ldots (2.6)$$

The average decay time τ_{av} in the biexponential fit is expressed as

$$\tau_{av} = \frac{A_1\tau_1^2 + A_2\tau_2^2}{A_1\tau_1 + A_2\tau_2} \quad \ldots (2.7)$$

In a bi-exponential decay curve fitting, τ_1 represents the fast decay associated with trap-assisted nonradiative recombination, while τ_2 represent the slower decay related to the free charge carriers' radiative recombination. A_i is the decay amplitude for the decay τ_i.

Hence, TRPL decay analysis is a powerful tool for studying the dynamics of excited states, providing valuable information for the development and optimization of a wide range of materials and devices.

2.5 Software used for the analysis of obtained data

2.5.1 FullProf Suite for the XRD analysis

FullProf Suite is one of the most frequently used software to fit the measured XRD pattern of the sample to predict the lattice parameters and subsequently the atomic positions [123]. To start the fitting iteration, initial guess of the structural parameters such as *a, b, c*, α, β, γ, etc., are required. For this, "X'pert HighScore Plus" software is used. The *a, b, c* values of the desired structure are obtained by LeBail fitting using the "FullProf Suite" software. Selection of background information and peak shape function are crucial and important to perfectly fit the parameters to the measured XRD pattern. For this, in all the LeBail fitting work, background information was set as "linear interpolation between a set of background points with refinable heights". At the same time peak shape function "Pseudo-Voigt" is selected. The fitting accuracy is quantified by the parameter R_{wp} (weighted profile R factor), R_{exp} (expected R factor), and χ^2 (goodness of fit) values [124]. The square of R_{wp} is defined as

$$R_{wp}^2 = \frac{\Sigma_i w_i (y_{C,i} - y_{O,i})^2}{\Sigma_i w_i (y_{O,i})^2} \quad \ldots (2.8)$$

Where w_i is the weight ($w_i = 1/\sigma^2[y_{O,i}]$, $[y_{O,i}] = \text{unceratinty estimate for } y_{O,i}$), $y_{C,i}$ is the computed intensity, $y_{O,i}$ is the observed intensity. Best possible R_{wp} quantity is called expected *R* factor (R_{exp}) and is mathematically represented as

$$R_{exp}^2 = \frac{N}{\Sigma_i w_i (y_{O,i})^2} \quad \ldots (2.9)$$

R_{wp} and R_{exp} define the goodness of fit χ^2, and is given as

$$\chi^2 = \frac{R_{wp}^2}{R_{exp}^2} = \frac{1}{N} \times \frac{\Sigma_i w_i (y_{C,i} - y_{O,i})^2}{\sigma^2 [y_{O,i}]} \quad \ldots (2.10)$$

Where, each symbols have their usual meaning defined above. To obtained the best fit of the parameters to the data least-square techniques is used.

In order to obtain the position (x, y, and z coordinates) of the atom, Rietveld refinement is performed. Initial guessed x, y, and z coordinates of the all the atoms are refined to perfectly fit the data to obtained the more accurate values. With the help of Rietveld refinement data, atomic bond angle, bond distance, and structure is obtained.

2.5.2 ImageJ software for TEM/SEM Image Analysis

The morphology of the particles of synthesized sample is obtained through the TEM and SEM analysis. Particle size and distribution profile of the micro/nanoparticles is calculated using the "ImageJ" software. The reference scale is set in "ImageJ" software according to the scale SEM/TEM image is taken. Average particle size and distribution profile is obtained by scaling number of particle seen in the image.

2.5.3 Color Calculator v7.77 for Luminescence Spectrum Analysis

Commission International de I′Eclairage (CIE) chromaticity analysis is one of the important tool for the chromaticity study of the luminescence spectrum for the applications such as color LED, WLED, color display devices, etc. [125]. Luminescence spectrum of the material is obtained by the photoluminescence spectrometer, then spectrum is explored for the different parametric study using software "Color Calculator v7.77". CIE 1931 chromaticity diagram gives the cumulative color coordinate (x, y) of the spectrum. Based on the (x, y) coordinate, suitability of the materials for the different applications such as color

LED, WLED, color display devices, etc., is preferred. Using this color purity and luminous efficacy of the optical radiation of the spectrum is also measured using this. Detailed discussion of all these parameters is given in Chapter 5. WLED is parametrized by color temperature, categorized into cool and warm light by calculating the color temperature value. Hence, this is one of the important tool to different parametric study for the lighting application.

2.5.3 OriginPro 9.0 for Graph Plotting

OriginPro is a comprehensive data analysis and graphing software used widely in science and engineering field. It offers the advanced data analysis facilities such as statistical analysis, curve fitting; high quality 2D and 3D graphing. This can be interfaced with other software such as MATLAB, LabVIEW, CIE, etc. It is user friendly and support various data format that include Excel, ASCII, HDF5, NetCDF, etc.

All the data obtained from characterizations such as XRD, UV-visible, FT-IR, photoluminescence spectroscopy, XPS, etc., are given to the graphical format using this software.